




## EFFECT OF PHOSPHORIC ACID ( $H_3PO_4$ ) ACTIVATION ON THE PREPARATION OF ACTIVATED CARBON FROM *GYMNOSTOMA RUMPHIANUM* WOOD

Soenandar Milian Tompunu Tengker<sup>1\*</sup>, Jeanne Maria Tuerah<sup>1</sup>, Pamela Lumingas<sup>1</sup>, Stefan Marco Rumengan<sup>1</sup>, and Alfrie Musa Rampengan<sup>2</sup>

<sup>1</sup> Department of Chemistry, Faculty of Mathematics, Natural Sciences, and Earth Sciences, Universitas Negeri Manado, Minahasa, Indonesia

<sup>2</sup> Department of Physics, Faculty of Mathematics, Natural Sciences, and Earth Sciences, Universitas Negeri Manado, Minahasa, Indonesia

ARTICLE INFO	ABSTRACT
<p><b>Keywords:</b> Gymnostoma rumphianum; Activated Charcoal; <math>H_3PO_4</math> Activator; XRD; TEM.</p> <p><b>Article History:</b> Received: 2025-08-04 Accepted: 2025-08-20 Published: 2025-08-31 doi:10.20961/jkpk.v10i2.107623</p>  <p>©2025 The Authors. This open-access article is distributed under a (CC-BY-SA License)</p>	<p>Smartphone-based digital image analysis (DIA) has emerged as an affordable and accessible tool for chemical analysis, particularly in colorimetry. While previous studies have largely emphasized quantitative measurements, this study investigates a machine learning-assisted DIA approach for qualitatively classifying synthetic food dyes. Digital images of nine dye solutions (Carmoisine, Sunset Yellow, Allura Red, Ponceau 4R, Tartrazine, Fast Green FCF, Brilliant Blue FCF, Quinoline Yellow WS, and Indigo Carmine) were captured under both controlled (closed) and ambient (open) lighting conditions using a smartphone camera. The images were processed to extract color features across multiple color spaces, including RGB, normalized RGB (rgb), HSL, and CIELAB. These features were then used to train a k-nearest neighbors (KNN) classifier for dye identification. The model achieved high-standard solutions performance, with accuracy exceeding 86% across all color spaces and lighting conditions. The classifier was tested on seven commercial food and health products to evaluate practical applicability. Among the evaluated color spaces, HSL consistently yielded the highest classification accuracy for commercial samples under both lighting conditions, with the open setup outperforming the controlled setup. These results highlight the feasibility of combining smartphone-based DIA with machine learning to provide a low-cost, portable, and reliable approach for qualitative colorimetric analysis, offering strong potential for food safety monitoring and on-site screening applications.</p>
<p>*Corresponding Author: <a href="mailto:soenandarmilianttengker@unima.ac.id">soenandarmilianttengker@unima.ac.id</a> <b>How to cite:</b> S. M. T. Tengker, J. M. Tuerah, P. Lumingas, S. M. Rumengan, and A. M. Rampengan, "Effect of Phosphoric Acid (<math>H_3PO_4</math>) Activation on the Preparation of Activated Carbon from <i>Gymnostoma Rumphianum</i> Wood," <i>Jurnal Kimia dan Pendidikan Kimia (JKPK)</i>, vol. 10, no. 2, pp. 336-250, 2025. [Online]. Available: <a href="https://doi.org/10.20961/jkpk.v10i2.107623">https://doi.org/10.20961/jkpk.v10i2.107623</a></p>	

### INTRODUCTION

Indonesia possesses exceptionally high biodiversity, including many tree species with strong potential as biomass energy sources. One species that remains underexplored but holds significant promise is the mountain casuarina (*Gymnostoma rumphianum* (Miq.) L.A.S. Johnson), locally

known as Roya wood. This species belongs to the Casuarinaceae family, which is characterized by hardwood properties, high durability, and suitability as a fuel source [1], [2].

Roya wood grows predominantly in tropical regions, particularly mountainous areas and rainforests [3], such as Sulawesi

and Maluku [4]. In Marawas Subdistrict, Minahasa Regency, North Sulawesi Province, local communities traditionally use Royia wood as a fuel for metal combustion, highlighting its high thermal potential. This finding aligns with previous studies reporting that Casuarinaceae family members exhibit low ash content and good combustibility even in a green condition, making them efficient fuel sources [2]. Despite this potential, the utilization of Royia wood is still limited to traditional charcoal production. Given its dense and durable structure, Royia wood shows considerable promise as a raw material for activated charcoal.

Activated charcoal is a porous material widely applied in water filtration, air purification, heavy metal adsorption, and the pharmaceutical and chemical industries. Its quality depends on the raw material type and processing conditions, with high-density and low-ash woods considered the most suitable feedstocks. According to [5], the production of activated charcoal generally involves three stages: drying, pyrolysis, and activation. The drying stage removes moisture, often under sunlight or with an oven, to prepare the raw material for pyrolysis. Pyrolysis, a thermochemical process conducted under high temperatures without oxygen, decomposes organic matter into solid, liquid, and gaseous products [6]. The final activation stage removes hydrocarbons from the charcoal surface to enhance porosity and adsorption properties [7]. This stage is commonly carried out through chemical activation using reagents such as  $\text{H}_3\text{PO}_4$ , KOH,  $\text{ZnCl}_2$ , or  $\text{H}_2\text{SO}_4$ .

Previous studies on other Casuarinaceae members, such as *Casuarina junghuhniana*, demonstrated that single and double activation with 2N KOH immersion for 1–5 days yielded iodine adsorption capacities of 317.25–507.60 mg/g and ash contents of 8–30%. These results did not meet the Indonesian National Standard (SNI 06-3730-1995), which requires a minimum iodine number of 750 mg/g and a maximum ash content of 10% [8]. Activation with HCl and NaOH for 24 hours resulted in moisture and ash contents of 2.97% and 3.92%, respectively [9]. Meanwhile, immersion in 6%  $\text{CH}_3\text{COOH}$  for 24 hours followed by heating at 105 °C produced charcoal with an iodine adsorption capacity of 761.58 mg/g [10].

Among the commonly used activating agents,  $\text{H}_3\text{PO}_4$  is particularly effective in producing highly porous activated charcoal [11], compared to KOH. This effect is attributed to  $\text{H}_3\text{PO}_4$  diffusion into the pores, which enhances acid hydrolysis and promotes pore development [12]. Furthermore,  $\text{H}_3\text{PO}_4$  penetrates deeply into pore structures, retaining the primary framework while facilitating the removal of alkali, alkaline earth metals, and iron impurities [13]. Studies have shown that  $\text{H}_3\text{PO}_4$  activation of jute-stick-based charcoal results in higher iodine adsorption capacity compared to activation with  $\text{H}_2\text{SO}_4$  or  $\text{ZnCl}_2$  [14]. Additionally,  $\text{H}_3\text{PO}_4$  is considered more environmentally friendly, requiring lower energy input and yielding higher carbon recovery [15].

Based on these considerations and the limited scientific studies investigating the potential of Royia wood, this research seeks

to evaluate the effect of  $\text{H}_3\text{PO}_4$  activation on the properties of activated charcoal derived from Roya wood. The study supports utilizing local biomass resources and advances the development of environmentally friendly, high-performance activated charcoal materials.

## METHODS

### 1. Materials and Equipment

This research was conducted at the Chemistry Laboratory, Faculty of Mathematics, Natural Sciences, and Earth Sciences, Manado State University, from November to December 2024.

The raw material used was Roya wood branches (RWB) collected from the forest area of Marawas Subdistrict, Minahasa Regency, North Sulawesi Province. Phosphoric acid ( $\text{H}_3\text{PO}_4$ , technical grade) at concentrations of 1%, 2%, and 3% served as the activating agent. A 0.1 N iodine ( $\text{I}_2$ ) solution was used to determine iodine adsorption capacity, while 0.1 N sodium thiosulfate pentahydrate ( $\text{Na}_2\text{S}_2\text{O}_3 \cdot 5\text{H}_2\text{O}$ , Alba Chemicals) was employed as the titration agent. Potassium iodide (KI, Alba Chemicals) was used as the iodine dissolving agent, and distilled water was used throughout the testing process.

The main instruments included a pyrolysis reactor for carbonization, a furnace (Ceramic Muffle Furnace FNC 7) for ash and volatile matter determination, an oven (Mettler UN 160) for drying and moisture content analysis, a universal indicator (Nesco pH paper 0–14), and a 100-mesh sieve. Structural characterization was conducted using an X-ray diffractometer (Bruker D6

Phaser) with a Cu anode radiation source ( $\lambda = 1.5406 \text{ \AA}$ ) to identify crystalline or amorphous phases and determine carbon purity. Particle size and d-spacing were analyzed using a Transmission Electron Microscope (TEM, JEOL JEM 1400) with an acceleration voltage of 40–120 kV and a  $\text{LaB}_6$ -cathode gun.

### 2. Sample Preparation

RWB samples were dried at room temperature, cut into approximately  $5 \times 7 \text{ cm}$  pieces, and divided into four smaller parts. The bark was removed prior to pyrolysis.

### 3. RWB pyrolysis.

The cleaned RWB samples were loaded into the pyrolysis reactor and heated for approximately 3 hours at  $365^\circ\text{C}$  (the maximum temperature of the reactor without temperature control). After cooling, the resulting charcoal was ground with a mortar and pestle, then sieved using a 100-mesh sieve [16].

### 4. Activation of RWB charcoal

Four RWB charcoal samples, each weighing 15 grams, were prepared and placed into 125 mL Erlenmeyer flasks. Each charcoal sample was labeled as: without activation (WA), 1%, 2%, and 3%. Then, 100 mL of  $\text{H}_3\text{PO}_4$  solution at concentrations of 1%, 2%, and 3% (v/v) (low concentrations to minimize the use of distilled water during neutralization) was added to each flask according to the concentration label. The same procedure was applied for the charcoal without activation, but distilled water was used as a substitute for  $\text{H}_3\text{PO}_4$ . All four samples were left to stand for 24 hours [16],

followed by filtration until no water dripped. After drying, the activated charcoal samples treated with 1%, 2%, and 3%  $H_3PO_4$  were washed with distilled water until reaching pH 7. Then, all four samples were dried in an oven at  $110 \pm 1^\circ C$  for 2 hours [16]. Once all activated charcoal samples were dry, physical and chemical properties were analyzed, which included: moisture content analysis using an oven at  $105^\circ C$  for 2 hours [17]; ash content analysis using a furnace at  $650^\circ C$  for 5 hours and 30 minutes [17]; volatile matter (VM) analysis using a furnace at  $950^\circ C$  for 7 minutes [5]; fixed carbon (FC) analysis calculated by subtracting the sum of ash content and VM from 100% [18]; and iodine adsorption capacity (IAC) analysis using sodium thiosulfate titration [17]. The samples were then characterized using X-ray Diffraction (XRD) and Transmission Electron Microscope (TEM) instruments.

$$\text{Moisture Content (\%)} = \frac{a-b}{a} \times 100\% \quad [7]$$

$$\text{Ash Content (\%)} = \frac{a-b}{a} \times 100\% \quad [19]$$

$$\text{VMC (\%)} = \frac{W_1 - W_2}{W_1} \times 100\% \quad [20]$$

$$\text{FCC \%} = 100\% - (\% \text{Ash content} + \% \text{VMC}) \quad [18]$$

$$\text{IAC (mg/g)} = A \frac{B \cdot N \cdot Na_2S_2O_3}{N \cdot \text{Iodine}} 126,93 \, df \quad [7]$$

Notation:

$a/W_1$	= Sample weight before heating (g)
$b/W_2$	= Sample weight after heating (g)
A	= Volume of Iodine solution (mL)
B	= Volume of Sodium thiosulfate used (mL)
df	= Dilution factor
a	= Mass of activated charcoal (g)

N	= Concentration of sodium thiosulfate (N)
N (Iodine)	= Concentration of Iodine (N)
126,93	= Amount of Iodine in 1 mL of Sodium thiosulfate solution

## RESULT AND DISCUSSION

### 1. Physical and Chemical Properties Analysis of RWB Activated Charcoal

#### a. Moisture Content

The moisture content analysis aims to determine the hygroscopic ability of activated charcoal based on the residual water retained in its pores after the pyrolysis and activation processes. The results of the moisture content analysis of RWB activated charcoal, both non-activated and  $H_3PO_4$ -activated, are presented in Table 1.

**Tabel 1.** Moisture Content of RWB-Based Activated Charcoal Without and With  $H_3PO_4$  Activation.

Sample	Value Moisture Content (%)	Specification SNI 06-3730-1995
TA	0,0504	
1	0,2631	Maximum 15%
2	0,2275	
3	0,1683	

Based on Table 1, all unactivated samples and  $H_3PO_4$ -activated at concentrations of 1%, 2%, and 3%—met the maximum moisture content requirement of 15% according to SNI 06-3730-1995 for activated carbon. The values ranged from 0.0504% to 0.1683%, indicating good compliance with the standard. The relationship between moisture content and  $H_3PO_4$  concentration is illustrated in Figure 1.

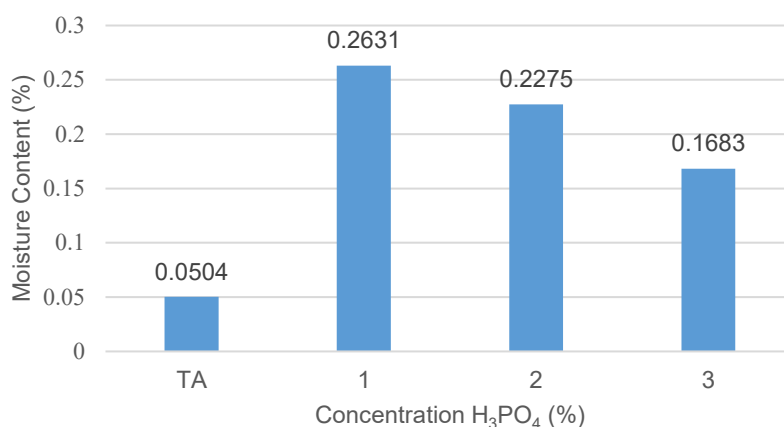


**Figure 1.** Moisture Content Analysis Percentage Graph

As shown in Figure 1, the moisture content of the unactivated RWB charcoal was lower than that of the  $H_3PO_4$ -activated samples. This increase can be attributed to introducing phosphate groups during activation, which render the surface of the charcoal more polar. Consequently, the surface exhibits a higher affinity for water molecules from the environment than unactivated samples [21].

However, the moisture content decreased as the  $H_3PO_4$  concentration increased from 1% to 3%. This trend suggests that stronger interactions between  $H_3PO_4$  and water molecules facilitated more effective water removal from the pores during heating, ultimately resulting in larger pore diameters in the activated charcoal [22].

Indrayani et al. [23] reported that lower moisture content correlates with a higher surface area, enhancing adsorption capacity. Similarly, several studies confirm that low moisture content increases the adsorption efficiency of activated charcoal [24]–[27].

**Table 2.** Ash Content of RWB-Based Activated Charcoal Without and With  $H_3PO_4$  Activation.

Sample	Value Ash Content (%)	Specification SNI 06-3730-1995
TA	2,4158	Maximum 10%
1	2,4625	
2	2,3981	
3	2,3321	

The moisture content obtained in this study was significantly lower than that reported by Hasanah et al. [16], who observed 12.63% in unactivated sugarcane bagasse, and by Prasetyo et al. [6], who found 8.16% in unactivated banana stem charcoal. These differences can be attributed to variations in raw material type and structural composition.

After the pyrolysis or activation process, the ash content analysis aims to determine the presence of inorganic minerals or metal oxides in the charcoal. The results of the ash content analysis of RWB-based activated charcoal, both non-activated and  $H_3PO_4$ -activated, are presented in Table 2.

Based on Table 2, the ash content results for samples without activation and activated with 1%, 2%, and 3%  $\text{H}_3\text{PO}_4$  have met the active carbon ash content standard of SNI 06-3730-1995, which has a maximum

limit of 10%, with ash contents of 2,4158%-2,3321%, respectively. The relationship between the ash content of non-activated and  $\text{H}_3\text{PO}_4$ -activated samples is shown in the graph in Figure 2.

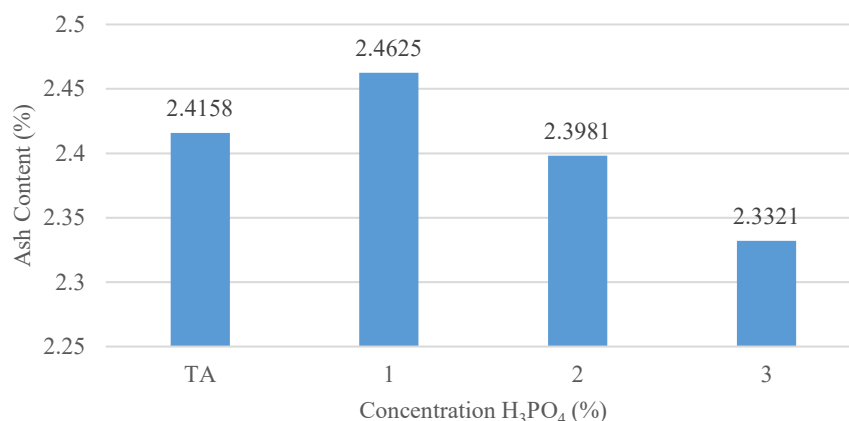


**Figure 2.** Graph of Ash Content Analysis Results.

Based on Figure 2, the ash content of unactivated charcoal slightly increased after activation with 1%  $\text{H}_3\text{PO}_4$ , but subsequently decreased with higher concentrations (2% and 3%). The initial increase in ash content at 1%  $\text{H}_3\text{PO}_4$  is likely due to incomplete mineral removal during the washing stage, resulting in more residual inorganic oxides trapped within the pores of the charcoal. However, at higher concentrations of  $\text{H}_3\text{PO}_4$ , the activator more effectively dissolved these minerals, leading to a reduction in ash content. This trend is consistent with the findings of Prasetyo et al. [6].

Previous studies using  $\text{H}_3\text{PO}_4$  activation, such as those conducted by Adawi et al. [28] and Dwityaningsih et al. [29], reported the opposite trend, where ash content increased with increasing  $\text{H}_3\text{PO}_4$  concentration. In contrast, the present study shows decreased ash content at higher

activator concentrations. According to Rini et al. [18],  $\text{H}_3\text{PO}_4$  plays an important role in corroding metallic elements within the charcoal, producing activated carbon with lower ash content. This is supported by Tiwow et al. [30], who found that inorganic minerals such as Fe, Mg, Ca, Al, and K often cover the pores of charcoal, thereby increasing the ash content.

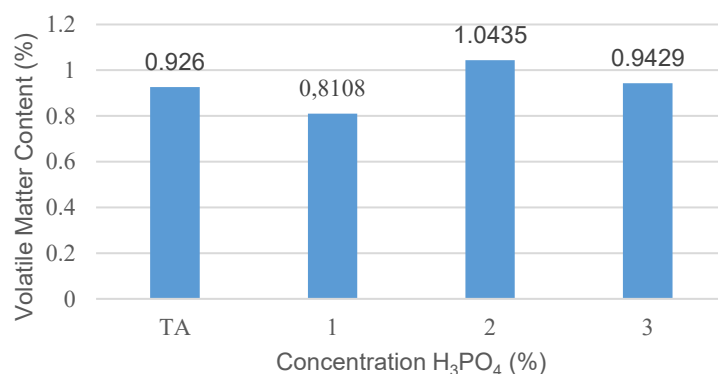
The differences in trends between this study and earlier works are likely due to variations in the raw materials used. For example, research by Wijaya et al. [31] using teak wood-based activated charcoal also demonstrated a decreasing ash content trend. Lower ash content is generally considered advantageous, as it indicates reduced inorganic residue and enhances the effectiveness of activated charcoal as an adsorbent [20].

**b. Volatile Matter Content****Table 3.** Volatile Matter Content of RWB-Based Activated Charcoal Without and With H<sub>3</sub>PO<sub>4</sub> Activation.

Sample	Value VMC (%)	Specification SNI 06-3730-1995
TA	0,9260	Maximum 25%
1	0,8108	
2	1,0435	
3	0,9429	

The volatile matter content (VMC) analysis was conducted to identify the presence of non-carbon compounds that

remain attached to the activated charcoal after the pyrolysis and activation processes. The results of the VMC analysis of RWB-based activated charcoal, both untreated and H<sub>3</sub>PO<sub>4</sub>-activated, are presented in Table 3. As shown in Table 3, both unactivated and H<sub>3</sub>PO<sub>4</sub>-activated samples met the SNI 06-3730-1995 standard for volatile matter in activated carbon, which requires a maximum value of 25%. The VMC values obtained ranged from 0.8108% to 1.0435%, well below the permissible limit. The relationship between untreated and activated samples is shown in Figure 3.

**Figure 3.** Percentage Graph of Volatile Matter Content Analysis Results: Kadar ZMM.

Based on Figure 3, the volatile matter content of RWB-based activated charcoal exhibited slight fluctuations after activation. The sample activated with 1% H<sub>3</sub>PO<sub>4</sub> showed a decrease in VMC compared to the untreated sample. This reduction is likely associated with the relatively higher moisture content at this concentration, which evaporated during heating at 950°C, thus lowering the final VMC.

The VMC increased slightly at higher concentrations (2% and 3% H<sub>3</sub>PO<sub>4</sub>). This trend may be attributed to the role of H<sub>3</sub>PO<sub>4</sub>

as an activating agent that provides partial protection against thermal decomposition, thereby reducing the release of volatile elements such as sulfur and nitrogen during heating. Similar findings were reported in previous studies, which indicated that activated charcoal generally contains 87–97% carbon, with the remainder composed of moisture, ash, sulfur, and nitrogen [18].

The VMC values obtained in this study were significantly lower than those reported by Prasetyo et al. [6], where unactivated banana stem-based charcoal exhibited a



VMC of 53.29%. This large difference highlights the influence of raw material type on volatile matter content. As noted in earlier works, high or low VMC indicates the extent of non-carbon compounds remaining on the surface of the activated charcoal, which can directly affect its adsorption performance.

### c. Fixed Carbon Content

The fixed carbon (FC) content analysis determines the amount of pure carbon after subtracting the ash and volatile matter contents. The results of the FC content analysis of RWB-based activated charcoal, both untreated and activated with  $\text{H}_3\text{PO}_4$ , are presented in Table 4.

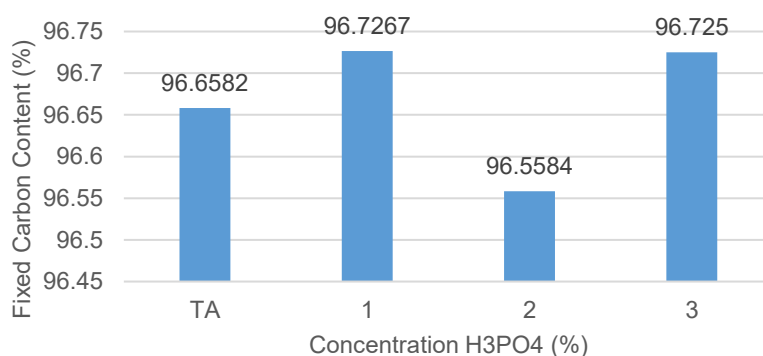


**Figure 4.** Percentage Graph of Fixed Carbon Content Analysis Results.

Based on Table 4, FC results for samples without activation and activated with 1%, 2%, and 3%  $\text{H}_3\text{PO}_4$  have met the SNI 06-3730-1995 standard for activated carbon, which requires a minimum of 65%, with FC values of 96,6582%-96,7250%, respectively. The relationship between the FC of samples without activation and those activated with  $\text{H}_3\text{PO}_4$  is shown in the graph in Figure 4. Based on Figure 4, an increase and a decrease in the fixed carbon (FC) content of RWB-based activated charcoal were observed. The high and low FC content of activated charcoal is influenced by the volatile matter (VM) and ash content. Furthermore, according to Hanavia et al. [32], the lower the VM and ash content, the higher the pure carbon content and the better the quality of the activated charcoal. According to

Adawi et al. [28], a higher pure carbon content results from a higher cellulose content in the raw material used to produce activated charcoal. A higher FC value indicates the activated charcoal's adsorption capacity [5].

**Table 4.** Fixed Carbon Content of RWB-Based Activated Charcoal Without and With  $\text{H}_3\text{PO}_4$  Activation.

Sample	Value FC (%)	Specification SNI 06-3730-1995
TA	96,6582	Maximum 65%
1	96,7267	
2	96,5584	
3	96,7250	

### d. Iodine Adsorption Capacity

The Iodine adsorption capacity analysis aims to determine the ability of



activated carbon to adsorb Iodine. The results of the iodine adsorption capacity (IAC) analysis for RWB activated carbon without activation and activated with  $H_3PO_4$  are shown in Table 5.

Based on Table 5, IAC results for samples without activation and activated with 1%, 2%, and 3%  $H_3PO_4$  have met the SNI 06-3730-1995 standard for activated carbon, which requires a minimum of 750 mg/g, with IAC values of 8885 mg/g-10535 mg/g/g, respectively. The relationship between the

IAC of samples without activation and those activated with  $H_3PO_4$  is shown in the graph in Figure 5.

**Table 5.** IAC Results of RWB-Based Activated Charcoal Without and With  $H_3PO_4$  Activation.

Sample	Value IAC (mg/g)	Specification SNI 06-3730-1995
TA	8885	Maximum 750 mg/g
1	9266	
2	9520	
3	10535	

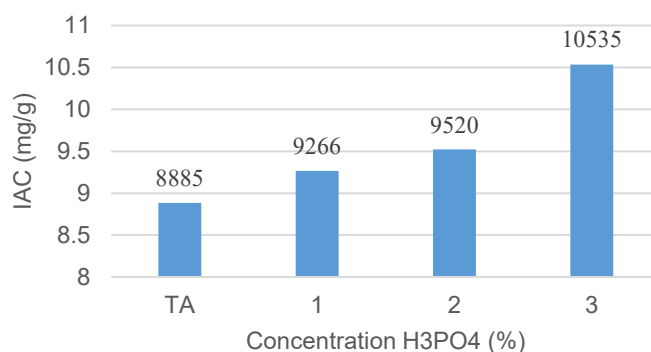


**Figure 5.** Percentage Graph of Iodine Number Analysis Results

Figure 5 shows that the higher the concentration of  $H_3PO_4$ , the greater the iodine adsorption value (IAC), due to a higher number of carbon atoms forming hexagonal crystalline carbon, which results in the formation of larger pores between the hexagonal crystal layers [33]. According to Saitun et al. [22], the increase in IAC is caused by removing impurities that previously blocked the pores, thus expanding the surface area of the activated charcoal and allowing more iodine to be adsorbed.

## 2. X-Ray Diffraction (XRD) Analysis

XRD analysis was conducted to identify the crystalline or amorphous phases, carbon purity, and d-spacing (interplanar distance) of RWB-based activated charcoal, untreated and activated with  $H_3PO_4$ . The XRD diffractograms of RWB activated charcoal without and with  $H_3PO_4$  activation are shown in Figure 6.

The XRD results for both untreated and  $H_3PO_4$ -activated samples reveal broad and non-sharp peaks, indicating the presence of an amorphous carbon structure. Similar findings were reported by Argianti et al. [34], who observed broad and non-distinct

peaks in coconut shell-based charcoal, characteristic of a predominantly amorphous structure. The amorphous phase is more advantageous than the crystalline phase for adsorption or filtration applications. The crystalline phase is more ordered and

structured, leaving limited space for adsorbate molecules. In contrast, the amorphous phase has a disordered structure, which can generate a wider range and larger pore sizes, thereby facilitating better adsorption of molecules.

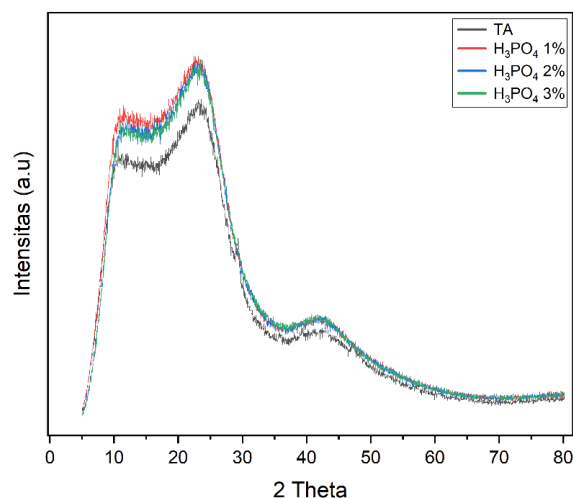


**Figure 6.** XRD Diffractograms of RWB-Based Activated Charcoal Without Activation (WA) and Activated with  $\text{H}_3\text{PO}_4$ .

In the untreated RWB charcoal sample, three broad diffraction peaks were observed within the ranges of  $9\text{--}14^\circ$ ,  $20\text{--}25^\circ$ , and  $35\text{--}50^\circ$ , along with one sharp peak in the  $25\text{--}30^\circ$  range. The sharp peak is suspected to originate from residual ash or mineral content from pyrolysis, as also noted in the study by Saban et al. [9]. After activation with  $\text{H}_3\text{PO}_4$ , the diffractograms of all three concentrations showed only three broad peaks within  $9\text{--}14^\circ$ ,  $20\text{--}25^\circ$ , and  $35\text{--}50^\circ$ , indicating that the addition of  $\text{H}_3\text{PO}_4$  at varying concentrations had no significant influence on the diffraction pattern of the RWB activated charcoal. This may be due to the relatively small difference in the concentration variations applied.

The diffraction peak in the  $9\text{--}14^\circ$  range of RWB-activated charcoal treated with

$\text{H}_3\text{PO}_4$  shifted, became broader, and showed increased intensity (d-spacing value from  $8.3570 \text{ \AA}$  to the range of  $7.3563\text{--}7.8063 \text{ \AA}$ ), indicating an increase in atomic layer disorder. At another peak in the  $20\text{--}25^\circ$  range (with a slight decrease in d-spacing from  $3.7374 \text{ \AA}$  to the range of  $3.6782\text{--}3.9032 \text{ \AA}$ ) and  $35\text{--}50^\circ$  (a significant decrease in d-spacing from  $2.9547 \text{ \AA}$  to the range of  $2.1236\text{--}2.2535 \text{ \AA}$ ), specific changes were observed, with peaks becoming broader and intensities increasing. This confirms that the structure became more amorphous, forming new pores on the surface of the RWB-activated charcoal. The formation of a more amorphous structure results in a wider range of pore sizes. These changes observed in the diffractogram of RWB activated charcoal indicate an increase in porosity and surface

area, which has implications for improved adsorption performance. These results align with the findings of Argianti et al. [34], who reported a similar diffraction pattern.

### 3. Transmission Electron Microscope (TEM) Analysis

The purpose of TEM analysis is to observe the morphological distribution and particle size of RWB activated charcoal without activation and activated with 1%  $H_3PO_4$ . The TEM images of RWB activated charcoal without and with 1%  $H_3PO_4$  activation are shown in Figure 7.

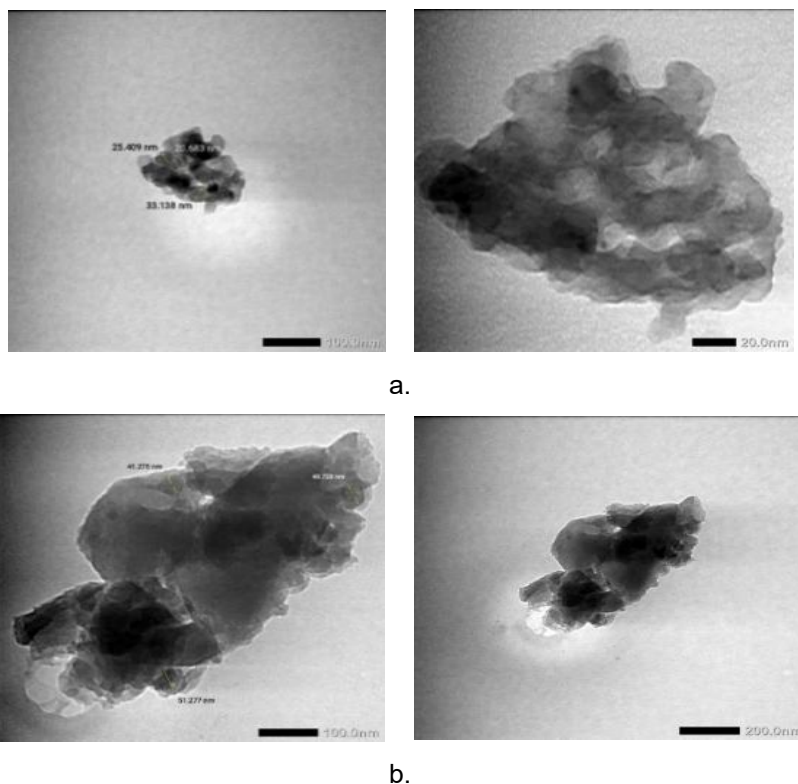


**Figure 7.** TEM Images of RWB Activated Charcoal (a) Without Activation (b) Activated with 1%  $H_3PO_4$ .

### CONCLUSION

The results of the physical and chemical property analyses of RWB activated charcoal, both non-activated and activated with 1%, 2%, and 3%  $H_3PO_4$ , showed moisture content of 0.0504%, 0.2631%, 0.2275%, and 0.1683%; ash content of 2.4158%, 2.4625%, 2.3981%, and 2.3321%; volatile matter content of 0.9260%, 0.8108%, 1.0435%, and 0.9429%; fixed carbon content of 96.6582%, 96.7267%, 96.5584%, and 96.7250%; and Iodine adsorption capacity of

8885 mg/g, 9266 mg/g, 9520 mg/g, and 10535 mg/g, respectively. All values meet the SNI 06-3730-1995 for activated charcoal. The XRD analysis showed that RWB activated charcoal samples, both non-activated and activated with 1%, 2%, and 3%  $H_3PO_4$ , exhibited amorphous characteristics. The non-activated RWB charcoal displayed three broad diffraction peaks within the ranges of 9–14°, 20–25°, and 35–50°, and one sharp peak around 25–30°. After  $H_3PO_4$  activation, only three broad peaks remained at 9–14°,

20–25°, and 35–50° for all three H<sub>3</sub>PO<sub>4</sub> concentration variations. The XRD patterns of the H<sub>3</sub>PO<sub>4</sub>-activated RWB charcoal showed increased intensity and broader peaks, indicating improved porosity and surface area. The d-spacing values of RWB activated charcoal for peak one were 2.9547 Å (Without activated), 2.1375 Å (1%), 2.1236 Å (2%), and 2.2535 Å (3%); for peak two, 3.7374 Å, 3.7023 Å, 3.6782 Å, and 3.9032 Å; and for peak three, 8.3570 Å, 7.4045 Å, 7.3563 Å, and 7.8063 Å, respectively. The TEM analysis showed that the particle size of non-activated RWB charcoal ranged from 20–33 nm, and increased to 41–51 nm after activation with 1% H<sub>3</sub>PO<sub>4</sub>. The increase in particle size after H<sub>3</sub>PO<sub>4</sub> activation indicates an enhancement in the porosity of the RWB activated charcoal.

## ACKNOWLEDGEMENT

The authors sincerely thank all parties who have provided support, assistance, and motivation throughout this research. Special thanks are extended to the Rector of Universitas Negeri Manado through the Institute for Research and Community Service (LPPM) for providing financial support and enabling this research to be carried out. It is hoped that this research will be beneficial and contribute positively to the advancement of scientific knowledge.

## REFERENCES

- [1] C. R. Schwintzer and J. D. Tjepkema, *The Biology of Frankia and Actinorhizal Plants*, California: Academic Press Inc, 1990.
- [2] W. D. Atmanto, W. W. Winarni, B. Primardiyatni, and S. Danarto, "Pertumbuhan Cabang Kayu Cemara pada Jarak Tanam yang Berbeda," *Life Science*, vol. 8, no. 2, pp. 126–137, 2019.
- [3] J. S. Berame, "Preliminary Results of Gymnosperm Species Inventory in Caraga Region XIII, Philippines," *International Scientific Indexing*, vol. 4, pp. 520–533, 2020.
- [4] I. F. Hanum and L. J. G. Van Der Maesen, *Plant Resources of South-East Asia 11: Auxiliary plants*, Jakarta: LIPI Press, 2007.
- [5] K. Sa'diyah, P. H. Suharti, N. Hendrawati, F. A. Pratamasari, and O. M. Rahayu, "Pemanfaatan serbuk gergaji kayu sebagai karbon aktif melalui proses pirolisis dan aktivasi kimia," *CHEESA: Chemical Engineering Research Articles*, vol. 4, no. 2, pp. 91–99, 2021. doi: [10.25273/cheesa.v4i2.8589.91-99](https://doi.org/10.25273/cheesa.v4i2.8589.91-99)
- [6] A. Prasetyo, R. D. Ratnani, and I. Riwayati, "Pemanfaatan limbah batang pisang (*Musa paradisiaca* L.) sebagai sumber karbon aktif teraktivasi dengan penerapan metode pirolisis dan asam fosfat (H<sub>3</sub>PO<sub>4</sub>)," *Prosiding Sains Nasional dan Teknologi*, vol. 14, no. 1, pp. 198–208, 2024.
- [7] N. F. Azzahra and D. Tanggasari, "Sifat Mutu Arang Aktif Kayu Bidara (*Ziziphus mauritiana*) Dengan Penambahan larutan H<sub>3</sub>PO<sub>4</sub> Berdasarkan Variasi Suhu Aktivasi," *Jurnal Biosistem Protech*, vol. 4, no. 1, pp. 36–44, 2024. doi: <https://doi.org/10.36761/fagi.v4i2.3583>
- [8] S. Jamilatun, E. N. Putri, Z. Arifah, and I. Mufandi, "The Effect of Single and Double Activation with Potassium Hydroxide 2N on Charcoal from Fir Wood (*Casuarina Junghuhniana*) Pyrolysis," *CHEMICA: Jurnal Teknik*

- Kimia*, vol. 7, no. 1, pp. 11–18, 2020. doi: [10.26555/chemica.v7i1.15651](https://doi.org/10.26555/chemica.v7i1.15651)
- [9] A. Saban, Jasruddin, and Husain, "Pengaruh Konsentrasi Aktivator (NaOH dan HCl) Terhadap Karakteristik Karbon Aktif Dari Tongkol Jagung," *Jurnal Sains dan Pendidikan Fisika (JSPF)*, vol. 19, no. 2, pp. 219–228, 2023.
- [10] M. Shellyanti and N. Komari, "Pembuatan dan Karakterisasi Arang Aktif dari Kayu Alaban (*Vitex Pinnata* L.) Menggunakan Asam Asetat," *Jurnal Natural Scientiae*, vol. 3, no. 2, pp. 33–37, 2023. doi: [10.20527/jns.v3i2.9892](https://doi.org/10.20527/jns.v3i2.9892)
- [11] I. Alouiz et al., "Elaboration of fibrous structured activated carbon from olive pomace via chemical activation and low-temperature pyrolysis," *Heliyon*, vol. 10, no. 20, pp. 1–13, 2024. doi: [10.1016/j.heliyon.2024.e38886](https://doi.org/10.1016/j.heliyon.2024.e38886)
- [12] A. M. S. Ngueabouo et al., "Strategy for optimizing the synthesis and characterization of activated carbons obtained by chemical activation of coffee husk," *Materials Advances*, vol. 3, no. 22, pp. 8361–8374, 2022.
- [13] P. Feng, J. Li, H. Wang, and Z. Xu, "Biomass-based activated carbon and activators: preparation of activated carbon from corncob by chemical activation with biomass pyrolysis liquids," *ACS Omega*, vol. 5, no. 37, pp. 24064–24072, 2020. doi: [10.1021/acsomega.0c03494](https://doi.org/10.1021/acsomega.0c03494)
- [14] M. N. Islam et al., "Preparation and characterization of activated carbon from jute stick by chemical activation: comparison of different activating agents," *Saudi Journal of Engineering and Technology*, vol. 7, no. 2, pp. 112–117, 2022. doi: [10.36348/sjet.2022.v07i02.008](https://doi.org/10.36348/sjet.2022.v07i02.008)
- [15] L. S. Daniel et al., "The production of activated carbon from *Acacia erioloba* seedpods via phosphoric acid activation method," *Bioresource Technology Reports*, vol. 23, 2023. doi: [10.1016/j.biteb.2023.101568](https://doi.org/10.1016/j.biteb.2023.101568)
- [16] H. Hasanah, R. Sirait, and R. Y. Lubis, "Pengaruh Konsentrasi Aktivator  $H_3PO_4$  Terhadap Karbon Aktif Ampas Tebu," *Journal Online of Physics*, vol. 8, no. 1, pp. 11–15, 2022.
- [17] D. Youlanda, S. Sitorus, and B. Yusuf, "Pemanfaatan arang aktif serbuk gergaji kayu bangkirai (*Shorea Lavefolia* Endert)," *Jurnal Atomik*, vol. 7, no. 1, pp. 18–21, 2022.
- [18] D. S. Rini et al., "Effect of activation temperature and  $H_3PO_4$  concentration on activated carbon from Asian Palmyra Palm Fronds," *Jurnal Multidisiplin Madani*, vol. 4, no. 6, pp. 720–728, 2024.
- [19] Y. Yuliawati and L. H. Rizaldi, "Sifat Mutu Arang Aktif Kayu Bidara (*Ziziphus mauritiana*) Dengan Larutan Kimia Natrium Hidroksida," *Food and Agro-industry Journal*, vol. 4, no. 2, pp. 1–10, 2023. doi: <https://doi.org/10.36761/fagi.v4i2.3583>
- [20] J. P. G. Sutapa et al., "Utilization of sapwood waste of fast-growing teak in activated carbon production," *Journal of the Korean Wood Science and Technology*, vol. 52, no. 2, pp. 118–133, 2024. doi: [10.5658/WOOD.2024.52.2.118](https://doi.org/10.5658/WOOD.2024.52.2.118)
- [21] H. Megherbi et al., "The effect of phosphoric acid on the properties of activated carbons from *Myrtus communis* leaves," *J. Mol. Struct.*, vol. 1321, no. 3, p. 140038, 2024. doi: [10.1016/j.molstruc.2024.140038](https://doi.org/10.1016/j.molstruc.2024.140038)

- [22] S. Saitun, U. Pato, and Y. Zalfiatri, "Konsentrasi Asam Fosfat ( $H_3PO_4$ ) Terhadap Karakteristik Arang Aktif Dari Tempurung Buah Nipah," *Sagu Journal: Agricultural Science and Technology*, vol. 23, no. 1, pp. 16–22, 2024.
- [23] Y. Indrayani et al., "Influence of activated charcoal addition on the properties of particleboard," *Jurnal Sylva Lestari*, vol. 10, no. 3, pp. 294–309, 2022. doi: [10.23960/jsl.v10i3.560](https://doi.org/10.23960/jsl.v10i3.560)
- [24] C. Bijang et al., "Synthesis and characterization of activated carbon from waste compedak fruit," *Jurnal Akademi Kimia*, vol. 11, no. 1, pp. 56–63, 2022.
- [25] A. Fitriansyah, H. Amir, and E. Elvinawati, "Karakterisasi adsorben karbon aktif dari sabut pinang," *Alotrop*, vol. 5, no. 1, pp. 42–54, 2021.
- [26] H. Haritha et al., "Production and characterization of activated charcoal from cocoa pod," M.S. thesis, KCAET Tavanur, Kerala Agricultural Univ., India, 2023.
- [27] P. H. Setyarini, F. Cendikia, and A. A. A. Sonief, "Enhance the quality of medical liquid waste," *International Journal of Integrated Engineering*, vol. 16, no. 2, pp. 144–152, 2024.
- [28] T. F. Adawi, I. M. L. Aji, and D. S. Rini, "Pengaruh Suhu dan Konsentrasi Asam Fosfat terhadap Arang Aktif Bambu Duri," *Jurnal Penelitian Kehutanan Faloak*, vol. 5, no. 1, pp. 62–73, 2021. doi: [10.20886/jpkf.2021.5.1.62-73](https://doi.org/10.20886/jpkf.2021.5.1.62-73)
- [29] R. Dwityaningsih et al., "Pengaruh variasi konsentrasi  $H_3PO_4$  terhadap karakteristik karbon aktif dari sekam padi," *Infotekmesin*, vol. 14, no. 1, pp. 98–104, 2023. doi: [10.35970/infotekmesin.v14i1.1641](https://doi.org/10.35970/infotekmesin.v14i1.1641)
- [30] V. A. Tiwow et al., "Pola Inframerah Arang Tempurung Kelapa Hasil Pemurnian," *Chem Prog.*, vol. 14, no. 2, pp. 116–123, 2021. doi: [10.35799/cp.14.2.2021.37191](https://doi.org/10.35799/cp.14.2.2021.37191)
- [31] L. S. Wijaya, D. S. Afuza, and E. Kurniati, "Arang Aktif Serbuk Kayu Jati Menggunakan Aktivator  $H_3PO_4$  dan Modifikasi  $TiO_2$ ," *Jurnal Teknik Kimia*, vol. 16, no. 2, pp. 73–79. doi: [10.33005/jurnal\\_tekkim.v16i2.3048](https://doi.org/10.33005/jurnal_tekkim.v16i2.3048)
- [32] M. S. Hanavia, C. I. A. Meliati, and L. Rubianto, "Pengaruh Suhu Pirolisis dan Konsentrasi Aktivator NaCl," *DISTILAT: Jurnal Teknologi Separasi*, vol. 8, no. 1, pp. 202–212, 2022. doi: [10.33795/distilat.v8i1.325](https://doi.org/10.33795/distilat.v8i1.325)
- [33] A. Budianto et al., "Physics and chemical activation to produce activated carbon from palm oil bunch waste," *IOP Conf. Ser.: Mater. Sci. Eng.*, vol. 10, pp. 1–8, 2021. doi: [10.1088/1757-899X/1010/1/012016](https://doi.org/10.1088/1757-899X/1010/1/012016)
- [34] K. N. Argianti, Y. Simbolon, E. B. Panggabean, Khairahmi, and M. K. Fahrozi, "Pengaruh Aktivasi Asam Dan Basa Terhadap Karakter Biochar Sebagai Katalis Heterogen," *Jurnal Matematika dan Ilmu Pengetahuan Alam*, vol. 5, no. 2, pp. 1–7, 2024.
- [35] M. S. Hossen, T. Islam, S. M. Hoque, A. Islam, M. M. Bashir, and G. Bhat, "Synthesis, activation, and characterization of carbon fiber precursor derived from jute fiber," *ACS Omega*, vol. 9, no. 33, pp. 35384–35393, 2024. doi: [10.1021/acsomega.4c01268](https://doi.org/10.1021/acsomega.4c01268)
- [36] A. E. Nemr, R. M. Aboughaly, A. El Sikaily, S. Ragab, M. S. Masoud, and M. S. Ramadan, "Utilization of sugarcane bagasse/ $ZnCl_2$  for

sustainable production of microporous nano-activated carbons of type I for toxic Cr (VI) removal from aqueous environment," *Biomass Conversion and Biorefinery*, vol. 13, no. 3, pp. 1581–1600, 2023.

orellana L.) viewed from temperature activation and impregnation ratio of  $H_3PO_4$ ," *EKSAKTA: Journal of Sciences and Data Analysis*, vol. 1, pp. 44–50, 2020. doi: [10.20885/EKSAKTA.vol1.iss1.art7](https://doi.org/10.20885/EKSAKTA.vol1.iss1.art7)

- [37] C. A. Riyanto, M. S. Ampri, and Y. Martono, "Synthesis and characterization of nano activated carbon from Annatto Peels (Bixa